Low-complexity time-varying frequency-shift equalization for doubly selective channels

Francesco Verde

Dipartimento di Ingegneria Elettrica e delle Tecnologie dell'Informazione
Università Federico II, Napoli, Italy,
Email: f.verde@unina.it

***Abstract*—This paper deals with the problem of designing linear time-varying (LTV) finite-impulse response equalizers for doubly selective channels. Specifically, we consider the frequency-domain representation of the LTV minimum mean-square error (MMSE) equalizer, which relies on the complex exponential basis expansion model of the time-varying channel impulse response and can be implemented as a parallel bank of linear time-invariant filters having, as input signals, different frequency-shift (FRESH) versions of the received data. We show that such a FRESH formulation allows to derive an effective low-complexity iterative version of the optimal LTV-MMSE equalizer, based on the steepest-descent method. Simulation results show that the proposed iterative equalizer ensures a very satisfactory tradeoff among complexity burden, convergence speed, and performance.**

I. Introduction

The design of reliable linear time-varying (LTV) estimation and detection strategies for wireless communication systems operating over time- and frequency-selective (so-called doubly selective) channels has been extensively studied in the literature, see, e.g., [1]–[8]. Such approaches rely on deterministic basis expansion models (BEMs), which allow one to express the channel impulse response as a superposition of time-varying basis functions with time-invariant coefficients. For instance, when the basis functions are complex exponentials (CEs) [1], the corresponding BEM is referred to as CE-BEM; an alternative BEM is the discrete prolate spheroidal (DPS) BEM (referred to as DPS-BEM) [9]. CE-BEM, when the frequency spacing of CEs is sufficiently small, and DPS-BEM approximate well [8] the Jakes statistical model.

Relying on the CE-BEM to represent doubly selective channels, serial and block finite-impulse response (FIR) LTV equalizers have been developed in [6], which are synthesized by resorting to both zero-forcing (ZF) and minimum mean-square error (MMSE) criteria. With reference to the same BEM used in [6], it has been derived in [7] the canonical frequency-domain representation of the minimal norm serial FIR-LTV ZF equalizer; the frequency-domain representation of LTV equalizers has the advantage that, unlike its time-domain counterpart, exhibits many similarities to linear time-invariant (LTI) filtering, wherein the time-varying component of the equalizer consists of computing frequency-shift (FRESH) [10] versions of the received data vector. On the basis of this FRESH representation, a suboptimal LTV-ZF equalizer has also been proposed in [7], which outperforms the serial ZF design of [6] at a lower computational cost (see also [8]). Recently, the authors in [8] have compared the MMSE variant of the FIR-FRESH ZF design of [7] with the Kalman equalizer, which is not a FIR filter. It has been shown in [8] that the FIR-FRESH MMSE equalizer is able to ensure almost the same performance of the Kalman filter, by involving, however, a higher computational burden.

In this paper, we propose an iterative version of the FRESH-MMSE equalizer, which relies on the steepest-descent (SD) method [11]. Specifically, we develop a novel recursive relation that turns out to be a generalization to doubly selective channels of conventional SD algorithm commonly employed for iteratively equalizing LTI channels. The proposed iterative approach allows one to significantly reduce both the design and implementation complexities of the FRESH-MMSE equalizer, with a slight performance penalty in the high signal-to-noise ratio (SNR) region.

Basic notations: Upper- and lower-case bold letters denote matrices and vectors; the superscripts $*$, T, H, and -1 denote the conjugate, the transpose, the Hermitian (conjugate transpose), and the inverse of a matrix; $\mathbb{C}$, $\mathbb{R}$, and $\mathbb{Z}$ are the fields of complex, real, and integer numbers; $\mathbb{C}^n$ $[\mathbb{R}^n]$ denotes the vector-space of all n-column vectors with complex [real] coordinates; similarly, $\mathbb{C}^{n\times m}$ $[\mathbb{R}^{n\times m}]$ denotes the vector-space of all the $n \times m$ matrices with complex [real] elements; $\mathbf{0}_n$, $\mathbf{O}_{n\times m}$, and $\mathbf{I}_n$ denote the n-column zero vector, the $n \times m$ zero matrix, and the $n \times n$ identity matrix; $\mathbf{A} = \text{diag}[\mathbf{A}_{11}, \mathbf{A}_{22}, \ldots, \mathbf{A}_{nn}]$ is the (block) diagonal matrix wherein $\{\mathbf{A}_{ii}\}_{i=1}^{n}$ are the block diagonal entries; $\bigtriangledown_{\mathbf{a}^*}(\cdot)$ represents the complex gradient operator with respect to $\mathbf{a}^* \in \mathbb{C}^{n\times m}$; $\mathrm{E}[\cdot]$ denotes statistical averaging and $\langle a(k)\rangle_K \stackrel{\triangle}{=} (1/K)\sum_{k=k_0}^{k_0+K-1} a(k)$ denotes temporal averaging of the sequence $a(k)$ over the time interval $\{k_0, k_0+1, \ldots, k_0+K-1\}$, with $k_0 \in \mathbb{Z}$; and, finally, $(\cdot)_P$, $\lceil\cdot\rceil$, $\otimes$, and $j \stackrel{\triangle}{=} \sqrt{-1}$ denote modulo-P operation, integer ceiling, Kronecker product, and imaginary unit.

II. System model and preliminaries

Let us consider a wireless high data-rate digital communication system, equipped with one transmitter antenna and

Also with Consorzio Nazionale Interuniversitario per le Telecomunicazioni (CNIT), Research Unit of Napoli. This work was partially supported by the Italian National Project "Harbour Traffic Optimization System" (HABITAT).

N receiver antennas, employing linear modulation with baud-rate $1/T_s$ and transmitting over a time- and frequency-selective channel. The complex envelope of the received signal at the nth antenna, after filtering, ideal carrier-frequency recovering, and baud-rate sampling, can be expressed as

$$r_n(k) = \sum_{\ell=0}^{L_h} h_n(k,\ell)\, s(k-\ell) + v_n(k) \tag{1}$$

where $s(k)$, with $k \in \mathbb{Z}$, is the sequence of the transmitted symbols, $h_n(k,\ell)$ denotes the *composite* impulse response of the L_h-order LTV channel corresponding to the nth receiver antenna, and $v_n(k)$ is additive noise at the output of the receiving filter employed at the nth antenna. The following customary assumptions will be considered in the sequel: **(a1)** the information symbols $s(k)$ are modeled as a sequence of independent and identically distributed (i.i.d.) zero-mean complex circular random variables, with variance $\sigma_s^2 \triangleq E[|s(k)|^2]$; **(a2)** the noise samples $\{v_n(k)\}_{n=1}^N$ are modeled as mutually independent zero-mean i.i.d. complex circular random sequences, with variance $\sigma_v^2 \triangleq \mathrm{E}[|v_n(k)|^2]$, statistically independent of $s(k)$ for each $k \in \mathbb{Z}$. In the sequel, we assume that σ_s^2 and σ_v^2 are exactly known at the receiver.

To allow for low-complexity detection strategies, we rely on the CE-BEM [6], whereby $h_n(k,\ell)$ is expressed as

$$h_n(k,\ell) = \sum_{q=-Q_h/2}^{Q_h/2} h_{q,n}(\ell)\, e^{j\frac{2\pi}{P}qk} \quad \text{for } k \in \mathcal{K} \text{ and } \ell \in \{0,1,\ldots,L_h\} \tag{2}$$

where $\mathcal{K} \triangleq \{k_0, k_0+1, \ldots, k_0+K-1\}$ is the observation window of finite length $K > 1$, with $k_0 \in \mathbb{Z}$, $P \geq K$, $Q_h \triangleq 2\lceil f_{\max} P T_s \rceil$, and $f_{\max}$ denotes the Doppler spread of the channel. When the CE-BEM is oversampled, i.e., $P > K$, model (2) and the DPS-BEM ensure a similar level of accuracy in approximating a Jakes' channel [8]. Hereinafter, we assume that, for each antenna, the coefficients $\{h_{q,n}(\ell)\}_{q=-Q_h/2}^{Q_h/2}$ are perfectly known at the receiver, $\forall \ell \in \{0,1,\ldots,L_h\}$, which can be estimated blindly [1]–[3], [12] or by employing training sequences [4], [5].

In order to compensate for the deleterious effects induced by both time- and frequency-selectivity of the transmission channel, we consider a causal LTV equalizer of order $L_e > 0$, whose input-output relationship is given by

$$y(k) = \mathbf{f}^{\mathrm{H}}(k)\, \mathbf{z}(k) \quad \text{for } k \in \mathcal{K} \tag{3}$$

where the vector $\mathbf{f}(k) \in \mathbb{C}^{N(L_e+1)}$ collects all the equalizer parameters, whereas the input vector is given by (see [7])

$$\mathbf{z}(k) \triangleq \begin{bmatrix} \mathbf{r}(k) \\ \mathbf{r}(k-1) \\ \vdots \\ \mathbf{r}(k-L_e) \end{bmatrix} = \left[\sum_{q=-Q_h/2}^{Q_h/2} \widetilde{\mathbf{H}}_q\, e^{j\frac{2\pi}{P}qk} \right] \mathbf{s}(k) + \mathbf{w}(k) \tag{4}$$

with $\mathbf{r}(k) \triangleq [r_1(k), r_2(k), \ldots, r_N(k)]^{\mathrm{T}} \in \mathbb{C}^N$, $\widetilde{\mathbf{H}}_q \triangleq \mathbf{J}_q\, \mathbf{H}_q$, $\mathbf{J}_q \triangleq \mathrm{diag}[\mathbf{I}_N, e^{-j\frac{2\pi}{P}q}\mathbf{I}_N, \ldots, e^{-j\frac{2\pi}{P}qL_e}\mathbf{I}_N]$, $\mathbf{H}_q \in \mathbb{C}^{N(L_e+1)\times(L_e+L_h+1)}$ being an upper-triangular block Toeplitz matrix whose first N rows are given by $[\mathbf{h}_q(0), \ldots, \mathbf{h}_q(L_h), \mathbf{0}_N, \ldots, \mathbf{0}_N]$, $\mathbf{h}_q(\ell) \triangleq [h_{q,1}(\ell), h_{q,2}(\ell), \ldots, h_{q,N}(\ell)]^{\mathrm{T}} \in \mathbb{C}^N$, for $\ell \in \{0,1,\ldots,L_h\}$, $\mathbf{s}(k) \triangleq [s(k), s(k-1), \ldots, s(k-L_e-L_h)]^{\mathrm{T}} \in \mathbb{C}^{L_e+L_h+1}$, and $\mathbf{w}(k) \triangleq [\mathbf{v}^T(k), \mathbf{v}^T(k-1), \ldots, \mathbf{v}^T(k-L_e)]^{\mathrm{T}} \in \mathbb{C}^{N(L_e+1)}$, where $\mathbf{v}(k) \triangleq [v_1(k), v_2(k), \ldots, v_N(k)]^{\mathrm{T}} \in \mathbb{C}^N$.

Our aim is to reliably estimate the transmitted symbol $s(k-d)$, with $d \in \{0,1,\ldots,L_e+L_h\}$ denoting a suitable equalization delay. In the absence of noise, under certain mild conditions, perfect or ZF symbol recovery can be obtained by using a LTV-ZF equalizer [7], which however, in the presence of noise, equalizes the channel at the price of noise enhancement. To better counteract the noise, we resort here to the LTV-MMSE equalizer given by

$$\mathbf{f}_{\text{mmse}}(k) = \sigma_s^2\, \mathbf{R}_{\mathbf{zz}}^{-1}(k)\, \widetilde{\mathbf{h}}_d(k) \quad \text{for } k \in \mathcal{K} \tag{5}$$

which minimizes the output mean-square error objective function $\mathrm{MSE}[\mathbf{f}(k)] \triangleq \mathrm{E}[|y(k)-s(k-d)|^2]$, $\forall k \in \mathcal{K}$, where $\mathbf{R}_{\mathbf{zz}}(k) \triangleq \mathrm{E}[\mathbf{z}(k)\, \mathbf{z}^{\mathrm{H}}(k)] \in \mathbb{C}^{N(L_e+1)\times N(L_e+1)}$ denotes the statistical time-varying correlation matrix of $\mathbf{z}(k)$, whereas $\widetilde{\mathbf{h}}_d(k)$ is the $(d+1)$th column of the channel matrix

$$\widetilde{\mathbf{H}}(k) \triangleq \sum_{q=-Q_h/2}^{Q_h/2} \widetilde{\mathbf{H}}_q\, e^{j\frac{2\pi}{P}qk} = \sum_{p=0}^{P-1} \boldsymbol{\mathcal{H}}^{(p)} e^{j\frac{2\pi}{P}pk} \tag{6}$$

where $\boldsymbol{\mathcal{H}}^{(p)}$ is shown at the top of the next page.

As it is apparent from (3) and (5), to obtain an estimate of the transmitted block of symbols, one has to evaluate the time-varying matrix $\mathbf{R}_{\mathbf{zz}}(k)$ for each value of $k \in \mathcal{K}$ and, then, compute the corresponding equalizer weight vector $\mathbf{f}_{\text{mmse}}(k)$, by performing K distinct matrix inversions. Therefore, the *time-domain* implementation of $\mathbf{f}_{\text{mmse}}(k)$ may lead to an high run-time complexity, especially for large values of the block size K. Motivated by this fact, we report in the next section the canonical *frequency-domain representation* of $\mathbf{f}_{\text{mmse}}(k)$ [7], [8], which allows us to derive an effective iterative low-complexity implementation of the LTV-MMSE equalizer.

III. Frequency-domain representation of the LTV-MMSE equalizer

Let us derive the frequency-domain representation of the LTV-MMSE equalizer (5). To do this, accounting for (6) and following [7], we observe that the correlation matrix $\mathbf{R}_{\mathbf{zz}}(k)$ admits the discrete Fourier series (DFS) expansion[1]

$$\mathbf{R}_{\mathbf{zz}}(k) = \sum_{p=0}^{P-1} \boldsymbol{\mathcal{R}}_{\mathbf{zz}}^{(p)} e^{j\frac{2\pi}{P}pk} \quad \text{for } k \in \mathbb{Z} \tag{8}$$

[1] Although (5) is valid only for $k \in \mathcal{K}$, without loss of generality, it is mathematically convenient, for obtaining the frequency-domain representations of $\mathbf{f}_{\text{mmse}}(k)$, to regard (5) as defined for all values of $k \in \mathbb{Z}$; obviously, in this case, only the values $\mathbf{f}_{\text{mmse}}(k_0), \mathbf{f}_{\text{mmse}}(k_0+1), \ldots, \mathbf{f}_{\text{mmse}}(k_0+K-1)$ of the obtained $\mathbf{f}_{\text{mmse}}(k)$ will be used for producing the equalizer output.

$$\boldsymbol{\mathcal{H}}^{(p)} \triangleq \begin{cases} \widetilde{\mathbf{H}}_p & \text{for } p \in \{0,1,\ldots,Q_h/2\}\,; \\ \mathbf{O}_{N(L_e+1)\times(L_h+L_e+1)} & \text{for } p \in \{Q_h/2+1, Q_h/2+2,\ldots,P-Q_h/2-1\}\,; \\ \widetilde{\mathbf{H}}_{p-P} & \text{for } p \in \{P-Q_h/2, P-Q_h/2+1,\ldots,P-1\}\,. \end{cases} \tag{7}$$

where its Fourier coefficients $\{\boldsymbol{\mathcal{R}}_{\mathbf{zz}}^{(p)}\}_{p=0}^{P-1}$ are referred to as the *cyclic correlation matrices* [10] of $\mathbf{z}(k)$. Since $\widetilde{\mathbf{H}}(k)$ and $\mathbf{R}_{\mathbf{zz}}(k)$ are periodic with period P, the optimal vector (5), when $k \in \mathbb{Z}$, is again periodic with period P and, thus, it can be expressed by means of its DFS expansion

$$\mathbf{f}_{\text{mmse}}(k) = \sum_{p=0}^{P-1} \mathbf{f}_{\text{mmse}}^{(p)}\, e^{j\frac{2\pi}{P}pk} \quad \text{for } k \in \mathbb{Z} \tag{9}$$

where $\{\mathbf{f}_{\text{mmse}}^{(p)}\}_{p=0}^{P-1}$ represent the Fourier coefficients of $\mathbf{f}_{\text{mmse}}(k)$. Let

$$\boldsymbol{\psi}_{\text{mmse}} \triangleq [(\mathbf{f}_{\text{mmse}}^{(0)})^{\text{T}}, (\mathbf{f}_{\text{mmse}}^{(1)})^{\text{T}}, \ldots, (\mathbf{f}_{\text{mmse}}^{(P-1)})^{\text{T}}]^{\text{T}} \in \mathbb{C}^{NP(L_e+1)} \tag{10}$$

collect all the Fourier coefficients of $\mathbf{f}_{\text{mmse}}(k)$, by substituting (8) and (9) in (5), it can be shown after straightforward algebraic manipulations (see also [7]) that

$$\boldsymbol{\psi}_{\text{mmse}} = \sigma_s^2\, \boldsymbol{\Phi}_{\mathbf{zz}}^{-1} \boldsymbol{\Theta}\, \mathbf{e}_d \tag{11}$$

where $\mathbf{e}_d \triangleq [\overbrace{0,\ldots,0}^{d},1,0,\ldots,0]^{\text{T}} \in \mathbb{R}^{L_e+L_h+1}$,

$$\boldsymbol{\Phi}_{\mathbf{zz}} \triangleq \begin{bmatrix} \boldsymbol{\mathcal{R}}_{\mathbf{zz}}^{(0)} & \boldsymbol{\mathcal{R}}_{\mathbf{zz}}^{(P-1)} & \ldots & \boldsymbol{\mathcal{R}}_{\mathbf{zz}}^{(2)} & \boldsymbol{\mathcal{R}}_{\mathbf{zz}}^{(1)} \\ \boldsymbol{\mathcal{R}}_{\mathbf{zz}}^{(1)} & \boldsymbol{\mathcal{R}}_{\mathbf{zz}}^{(0)} & \ldots & \boldsymbol{\mathcal{R}}_{\mathbf{zz}}^{(3)} & \boldsymbol{\mathcal{R}}_{\mathbf{zz}}^{(2)} \\ \vdots & \vdots & \vdots & \vdots & \vdots \\ \boldsymbol{\mathcal{R}}_{\mathbf{zz}}^{(P-1)} & \boldsymbol{\mathcal{R}}_{\mathbf{zz}}^{(P-2)} & \ldots & \boldsymbol{\mathcal{R}}_{\mathbf{zz}}^{(1)} & \boldsymbol{\mathcal{R}}_{\mathbf{zz}}^{(0)} \end{bmatrix} \tag{12}$$

is a $NP(L_e+1) \times NP(L_e+1)$ *block circulant* matrix and $\boldsymbol{\Theta} \triangleq [(\boldsymbol{\mathcal{H}}^{(0)})^{\text{T}}, (\boldsymbol{\mathcal{H}}^{(1)})^{\text{T}}, \ldots, (\boldsymbol{\mathcal{H}}^{(P-1)})^{\text{T}}]^{\text{T}} \in \mathbb{C}^{NP(L_e+1)\times(L_e+L_h+1)}$. Eq. (11) is the *equivalent* frequency-domain representation of the LTV-MMSE equalizer (5). Relying on this alternative representation, and accounting for (3), (9) and (11), the output $y_{\text{mmse}}(k)$ of the LTV-MMSE equalizer $\mathbf{f}_{\text{mmse}}(k)$ assumes the form

$$\begin{aligned} y_{\text{mmse}}(k) &= \mathbf{f}_{\text{mmse}}^{\text{H}}(k)\, \mathbf{z}(k) = \left[\sum_{p=0}^{P-1} \mathbf{f}_{\text{mmse}}^{(p)}\, e^{j\frac{2\pi}{P}pk}\right]^{\text{H}} \mathbf{z}(k) \\ &= \boldsymbol{\psi}_{\text{mmse}}^{\text{H}}\, \widetilde{\mathbf{z}}(k) \quad \text{for } k \in \mathcal{K} \end{aligned} \tag{13}$$

where $\widetilde{\mathbf{z}}(k) \triangleq \boldsymbol{\zeta}(k) \otimes \mathbf{z}(k) \in \mathbb{C}^{NP(L_e+1)}$ is given by

$$\widetilde{\mathbf{z}}(k) = \boldsymbol{\mathcal{H}}_{\text{circ}}\, \widetilde{\mathbf{s}}(k) + \widetilde{\mathbf{w}}(k) \tag{14}$$

with

$$\boldsymbol{\mathcal{H}}_{\text{circ}} \triangleq \begin{bmatrix} \boldsymbol{\mathcal{H}}^{(0)} & \boldsymbol{\mathcal{H}}^{(P-1)} & \ldots & \boldsymbol{\mathcal{H}}^{(2)} & \boldsymbol{\mathcal{H}}^{(1)} \\ \boldsymbol{\mathcal{H}}^{(1)} & \boldsymbol{\mathcal{H}}^{(0)} & \ldots & \boldsymbol{\mathcal{H}}^{(3)} & \boldsymbol{\mathcal{H}}^{(2)} \\ \vdots & \vdots & \vdots & \vdots & \vdots \\ \boldsymbol{\mathcal{H}}^{(P-1)} & \boldsymbol{\mathcal{H}}^{(P-2)} & \ldots & \boldsymbol{\mathcal{H}}^{(1)} & \boldsymbol{\mathcal{H}}^{(0)} \end{bmatrix} \tag{15}$$

being a $NP(L_e+1) \times P(L_e+L_h+1)$ *block circulant* matrix,

$$\boldsymbol{\zeta}(k) \triangleq [1, e^{-j\frac{2\pi}{P}k}, \ldots, e^{-j\frac{2\pi}{P}(P-1)k}]^T \in \mathbb{C}^P \tag{16}$$

$$\widetilde{\mathbf{s}}(k) \triangleq \boldsymbol{\zeta}(k) \otimes \mathbf{s}(k) \in \mathbb{C}^{P(L_e+L_h+1)} \tag{17}$$

$$\widetilde{\mathbf{w}}(k) \triangleq \boldsymbol{\zeta}(k) \otimes \mathbf{w}(k) \in \mathbb{C}^{NP(L_e+1)}\,. \tag{18}$$

Eq. (13) describes the FRESH representation [10] of $\mathbf{f}_{\text{mmse}}(k)$, for which the LTV-MMSE equalizer is represented in the frequency-domain as a parallel bank of LTI equalizers, each of one driven by a different frequency-shifted version of $\mathbf{z}(k)$, and the output $y_{\text{mmse}}(k)$ is formed by summing the outputs of the equalizers.

IV. Iterative LTV-MMSE equalization

When batch algorithms are used to compute $\boldsymbol{\psi}_{\text{mmse}}$ in (11), the *design* complexity of the LTV-MMSE equalizer is dominated by the matrix inversion $\boldsymbol{\Phi}_{\mathbf{zz}}^{-1}$, which requires $\mathcal{O}[N^3P^3(L_e+1)^3]$ floating point operations (flops); such a complexity may be unsustainable for large values of P.

At this point, our aim is to synthesize $\boldsymbol{\psi}_{\text{mmse}}$ with a more manageable computational complexity. To do this, we first observe that, in light of (7), the cyclic correlation matrices exhibit the structure reported at the top of the next page, which shows that one has to evaluate *only* Q_h+1 of the P cyclic correlation matrices $\{\boldsymbol{\mathcal{R}}_{\mathbf{zz}}^{(q)}\}_{q=0}^{P-1}$. In its turn, this implies that $\boldsymbol{\Phi}_{\mathbf{zz}}$ given by (12) exhibits a large sparse structure, which makes iterative methods especially attractive for computing $\boldsymbol{\psi}_{\text{mmse}}$. Although several sophisticated approaches can be used to iteratively estimate $\boldsymbol{\psi}_{\text{mmse}}$, we resort here to the SD method [11] since it leads to simple adaptation rules.

Before proceeding further, two key observations are in order regarding the frequency-domain representation of the LTV-MMSE equalizer. First, accounting for (14) and (19), it is readily verified that (12) coincides with the time-averaged statistical correlation matrix of $\widetilde{\mathbf{z}}(k)$, that is, $\boldsymbol{\Phi}_{\mathbf{zz}} = \langle \text{E}[\widetilde{\mathbf{z}}(k)\, \widetilde{\mathbf{z}}^{\text{H}}(k)] \rangle_K$. Second, it is seen that $\boldsymbol{\psi}_{\text{mmse}}$ in (11) can also be regarded as the solution of a different optimization criterion, i.e., the minimization of the time-averaged mean-square error

$$\begin{aligned} \text{TAMSE}(\boldsymbol{\psi}) &\triangleq \langle \text{E}[|\boldsymbol{\psi}^{\text{H}}\, \widetilde{\mathbf{z}}(k) - s(k-d)|^2] \rangle_K \\ &= \boldsymbol{\psi}^{\text{H}}\, \boldsymbol{\Phi}_{\mathbf{zz}}\, \boldsymbol{\psi} - \sigma_s^2\, \boldsymbol{\psi}^{\text{H}}\, \boldsymbol{\Theta}\, \mathbf{e}_d - \sigma_s^2\, \mathbf{e}_d^{\text{T}}\, \boldsymbol{\psi}^{\text{H}}\, \boldsymbol{\Theta}\, \mathbf{e}_d + \sigma_s^2 \end{aligned} \tag{20}$$

whose minimum value

$$\begin{aligned} \text{TAMSE}_{\text{min}} &\triangleq \text{TAMSE}(\boldsymbol{\psi}_{\text{mmse}}) \\ &= \sigma_s^2 \left(1 - \sigma_s^2\, \mathbf{e}_d^{\text{T}}\, \boldsymbol{\Theta}^H\, \boldsymbol{\Phi}_{\mathbf{zz}}^{-1}\, \boldsymbol{\Theta}\, \mathbf{e}_d\right)\,. \end{aligned} \tag{21}$$

coincides with $\langle \text{MSE}[\mathbf{f}_{\text{mmse}}(k)] \rangle_K$.

$$\boldsymbol{\mathcal{R}}_{\mathbf{zz}}^{(q)} = \begin{cases} \sigma_s^2 \sum\limits_{p=0}^{P-1} \boldsymbol{\mathcal{H}}^{(p)} \, [\boldsymbol{\mathcal{H}}^{(p)}]^{\mathrm{H}} + \sigma_v^2 \, \mathbf{I}_{N(L_e+1)} & \text{for } q = 0 \, ; \\ \sigma_s^2 \sum\limits_{p=0}^{P-1} \boldsymbol{\mathcal{H}}^{(p)} \, [\boldsymbol{\mathcal{H}}^{(p-q)_P}]^{\mathrm{H}} & \text{for } q \in \{1, 2, \ldots, Q_h\} \, ; \\ \mathbf{O}_{N(L_e+1) \times N(L_e+1)} & \text{for } q \in \{Q_h+1, Q_h+2, \ldots, P-Q_h-1\} \, ; \\ [\boldsymbol{\mathcal{R}}_{\mathbf{zz}}^{(P-q)}]^{\mathrm{H}} & \text{for } q \in \{P-Q_h, P-Q_h+1, \ldots, P-1\} \, . \end{cases} \tag{19}$$

At this point, we are in the position of developing the SD recursive rule of $\boldsymbol{\psi}_{\text{mmse}}$. To this end, let $\mathbf{f}^{(p)}(k)$ denote an estimate at iteration k of the pth optimal Fourier coefficient $\mathbf{f}_{\text{mmse}}^{(p)}$ in (10), for $p \in \{0, 1, \ldots, P-1\}$, the vector

$$\boldsymbol{\psi}(k) \triangleq [\{\mathbf{f}^{(0)}(k)\}^{\mathrm{T}}, \{\mathbf{f}^{(1)}(k)\}^{\mathrm{T}}, \ldots, \{\mathbf{f}^{(P-1)}(k)\}^{\mathrm{T}}]^{\mathrm{T}} \tag{22}$$

is an estimate at iteration k of $\boldsymbol{\psi}_{\text{mmse}}$ given by (11). According to the method of SD [11], the updated value of $\boldsymbol{\psi}_{\text{mmse}}$ at iteration $k+1$ is computed by using the iterative relation

$$\begin{aligned} \boldsymbol{\psi}(k+1) &= \boldsymbol{\psi}(k) - \mu \, \nabla_{\boldsymbol{\psi}^*(k)} \{\text{TAMSE}[\boldsymbol{\psi}(k)]\} \\ &= \boldsymbol{\psi}(k) + \mu \, \left[\sigma_s^2 \, \boldsymbol{\Theta} \, \mathbf{e}_d - \boldsymbol{\Phi}_{\mathbf{zz}} \, \boldsymbol{\psi}(k)\right] \end{aligned} \tag{23}$$

where $\mu > 0$ is the step-size parameter. By exploiting the sparse and block circulant nature of $\boldsymbol{\Phi}_{\mathbf{zz}}$, it follows from (23) that the updated value $\mathbf{f}^{(p)}(k+1)$ of the estimate of $\mathbf{f}_{\text{mmse}}^{(p)}$ at iteration $k+1$ is computed by resorting to the recursive rule

$$\mathbf{f}^{(p)}(k+1) = \mathbf{f}_s^{(p)}(k) - \mathbf{f}_c^{(p)}(k) \quad \text{for } k \in \mathcal{K} \tag{24}$$

where

$$\mathbf{f}_s^{(p)}(k) = \mathbf{f}^{(p)}(k) + \mu \left[\sigma_s^2 \, \boldsymbol{\mathcal{H}}^{(p)} \, \mathbf{e}_d - \boldsymbol{\mathcal{R}}_{\mathbf{zz}}^{(0)} \, \mathbf{f}^{(p)}(k)\right] \tag{25}$$

is referred to as the *the stationary component*, whereas

$$\mathbf{f}_c^{(p)}(k) = \mu \sum_{\substack{m=-Q_h \\ m \neq 0}}^{Q_h} \boldsymbol{\mathcal{R}}_{\mathbf{zz}}^{(m)_P} \, \mathbf{f}^{(p-m)_P}(k) \, , \tag{26}$$

is referred to as the *cyclic component*. It is worthwhile to note that the stationary component depends only on the value $\mathbf{f}^{(p)}(k)$ of the pth Fourier coefficient at time k; in contrast, the cyclic component at time k depends on the $2\,Q_h$ Fourier coefficients $\mathbf{f}^{(p-m)_P}(k)$, for $m \in \{-Q_h, -Q_h+1, \ldots, Q_h\} - \{0\}$. It is worth noting that, for a time-invariant channel (i.e., $Q_h = 0$), it results that $\mathbf{f}_c^{(p)}(k) = 0$ and, thus, the recursive relation (24) boils down to the conventional SD algorithm commonly employed for iteratively equalizing LTI channels. Strictly speaking, the cyclic component (26) represents the *correction* that must be applied to the conventional SD algorithm in order to account for the LTV nature of the channel. It is apparent that use of (24)-(26) to estimate the Fourier coefficients in the DFS of $\mathbf{f}_{\text{mmse}}(k)$ leads to a significant reduction of the design complexity of the LTV-MMSE equalizer.

With reference to the *implementation complexity*, we observe that a significant saving can be obtained if the equalizer

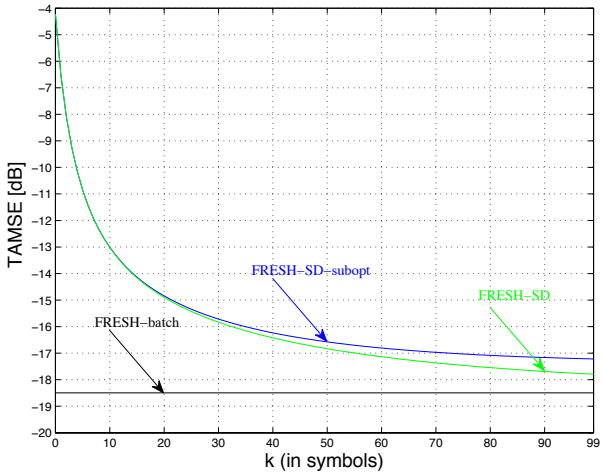

Figure 1. TAMSE versus number of iterations.

weight vector is represented with a series expansion by using only a small number of Fourier coefficients. More precisely, we can consider the following suboptimal equalizer

$$\widehat{\mathbf{f}}_{\text{mmse}}(k) = \sum_{p=-Q_e/2}^{Q_e/2} \widehat{\mathbf{f}}_{\text{mmse}}^{(p)} \, e^{j\frac{2\pi}{P}pk} \quad \text{for } k \in \mathbb{Z} \tag{27}$$

with

$$\widehat{\mathbf{f}}_{\text{mmse}}^{(p)} \triangleq \begin{cases} \mathbf{f}_{\text{mmse}}^{(p)} & \text{for } p \in \{0, 1, \ldots, Q_e/2\} \, ; \\ \mathbf{f}_{\text{mmse}}^{(P+p)} & \text{for } p \in \{-1, -2, \ldots, -Q_e/2\} \, ; \end{cases} \tag{28}$$

where only[2] $Q_h + 1 < Q_e + 1 < P$ Fourier coefficients are employed. Consequently, the FRESH implementation of $\widehat{\mathbf{f}}_{\text{mmse}}(k)$ is only composed by $Q_e + 1$ LTI equalizers, whose outputs are summed obtaining thus the overall output

$$\widehat{y}_{\text{mmse}}(k) = \widehat{\mathbf{f}}_{\text{mmse}}^{H}(k) \, \mathbf{z}(k) = \widehat{\boldsymbol{\psi}}_{\text{mmse}}^{H} \, \overline{\mathbf{z}}(k) \quad \text{for } k \in \mathcal{K} \tag{29}$$

where

$$\begin{aligned} \widehat{\boldsymbol{\psi}}_{\text{mmse}} \triangleq [(\widehat{\mathbf{f}}_{\text{mmse}}^{(0)})^T, (\widehat{\mathbf{f}}_{\text{mmse}}^{(1)})^T, \ldots, (\widehat{\mathbf{f}}_{\text{mmse}}^{(Q_e/2)})^T, (\widehat{\mathbf{f}}_{\text{mmse}}^{(P-Q_e/2)})^T, \\ \ldots, (\widehat{\mathbf{f}}_{\text{mmse}}^{(P-1)})^T]^T \in \mathbb{C}^{N(L_e+1)(Q_e+1)} \end{aligned} \tag{30}$$

[2]It is assumed in the sequel that Q_e is an even integer number.

and

$$\overline{\mathbf{z}}(k) \stackrel{\triangle}{=} \boldsymbol{\xi}(k) \otimes \mathbf{z}(k) \in \mathbb{C}^{N(L_e+1)(Q_e+1)} \tag{31}$$

$$\boldsymbol{\xi}(k) \stackrel{\triangle}{=} [1, e^{-j\frac{2\pi}{P}k}, \ldots, e^{-j\frac{2\pi}{P}(Q_e/2)k}, e^{-j\frac{2\pi}{P}(P-Q_e/2)k}, \ldots, e^{-j\frac{2\pi}{P}(P-1)k}]^T \in \mathbb{C}^{Q_e+1}. \tag{32}$$

Using the suboptimal LTV equalizer given by (27)-(28), where the relevant Fourier coefficients are calculated through (24)-(26) one can obtain a channel equalization procedure with a manageable design and implementation complexity.

V. Simulation results

In this section, the TAMSE performance of the proposed iterative FRESH-SD version of the LTV-MMSE equalizer (referred to as FRESH-SD), whose P Fourier coefficients in the DFS expansion of $\mathbf{f}_{\text{mmse}}(k)$ [see (9)] are calculated through (24)-(26), is investigated by means of Monte Carlo computer simulations, and compared with the TAMSE performance of its batch counterpart given by (11) (referred to as FRESH-batch), as well as with that of the suboptimal FRESH-SD equalizer (referred to as FRESH-SD-subopt) with input-otput relationship given by (29), whose $Q_e + 1$ Fourier coefficients in the DFS expansion (27) are calculated through (24)-(26), by setting $Q_e = 40$.

The transmitted symbols $s(k)$ are drawn from a QPSK constellation, and the composite channels $\{h_n(k,\ell)\}_{n=1}^{N}$ are 3rd-order (i.e., $L_h = 3$) random LTV systems, generated as in [7], with symbol period $T_s = 160\,\mu$s and maximum Doppler spread $f_{\max} = 100$ Hz. The block size is equal to $K = 100$ and $P = 2\,K$, which leads to $Q_h = 2\,\lceil f_{\max}\,P\,T_s \rceil = 8$. The number of receiver antennas is set to $N = 2$, whereas the order of all the considered equalizers is equal to $L_e = 6$ and the equalization delay d is chosen as the integer value nearest to $(L_h + L_e)/2$. The SNR is defined as in [7]. With reference to the SD-based algorithms, we set $\mathbf{f}^{(p)}(k_0 - 1) = \mathbf{0}_{N(L_e+1)}$ and $\mu = 1.9/\lambda_{\max}(\boldsymbol{\Phi}_{\mathbf{zz}})$, where $\lambda_{\max}(\boldsymbol{\Phi}_{\mathbf{zz}})$ is the largest eigenvalue of $\boldsymbol{\Phi}_{\mathbf{zz}}$. All the results are obtained by carrying out 10^3 independent trials, with each run using a different set of channel parameters.

Fig. 1 depicts the *learning curves* of the "FRESH-SD" and "FRESH-SD-subopt" equalizers versus the number of iterations, with SNR $= 20$ dB. It is seen that the performances of both the SD-based equalizers quickly improve as the number of iterations grows, by closely approaching the TAMSE value of the "FRESH-batch" equalizer. Remarkably, the learning curve of the "FRESH-SD-subopt" equalizer, which involves only $Q_e + 1 = 41$ Fourier coefficients, strictly follows that of its "FRESH-SD" counterpart, which instead employs all the $P = 2\,K = 200$ Fourier coefficients in the DFS expansion of $\mathbf{f}_{\text{mmse}}(k)$ and, thus, exhibits much greater design and implementation complexities.

In Fig. 2, we evaluate the TAMSE performances of the considered equalizers as a function of SNR. From this figure, we can observe that, for SNR $\leq$ 20 dB, the proposed SD-based equalizers perform very close to their "FRESH-batch" counterpart. Even though the performance penalty of the "FRESH-SD" and "FRESH-SD-subopt" equalizers with respect to the "FRESH-batch" one becomes more pronounced for larger values of the SNR, it is noteworthy that such iterative equalizers are able of achieving a TAMSE value of about -20 dB for SNR $= 30$ dB.

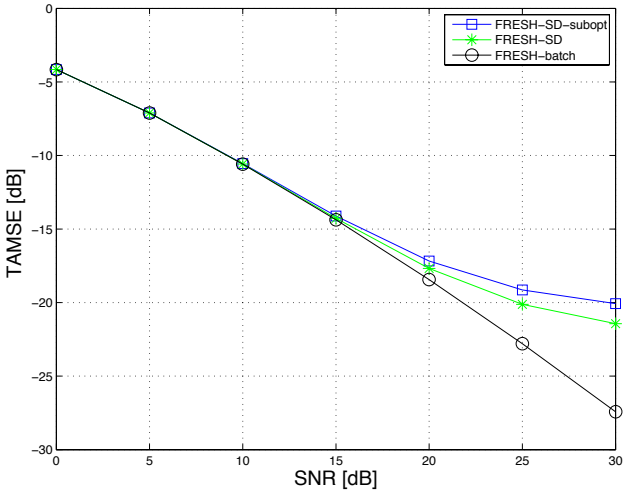

Figure 2. TAMSE versus SNR.

References

[1] G.B. Giannakis and C. Tepedelenlioğlu, "Basis expansion models and diversity techniques for blind identification and equalization of time-varying channels," *Proc. IEEE*, pp. 1969–1986, Oct. 1998.

[2] J.K. Tugnait and W. Luo, "Linear prediction error method for blind identification of periodically time-varying channels," *IEEE Trans. Signal Processing*, pp. 3070–3082, Dec. 2002.

[3] J.K. Tugnait and W. Luo, "Blind identification of time-varying channels using multispep linear predictors," *IEEE Trans. Signal Processing*, pp. 1739–1749, June 2004.

[4] W. Luo and J.K. Tugnait, "Semi-blind time-varying channel estimation using superimposed training," in *Proc. of Int. Conf. on Acoustic, Speech, and Signal Processing*, Montreal, Canada, pp. 797–800, May 2004.

[5] G. Leus, "On the estimation of rapidly time-varying channels," in *Proc. of Eur. Signal Processing Conf.*, Vienna, Austria, pp. 120–123, Sep. 2004.

[6] I. Barhumi, G. Leus, and M. Moonen, "Time-varying FIR equalization for doubly selective channels," *IEEE Trans. Wireless Commun.*, pp. 202–214, Jan. 2005.

[7] F. Verde, "Frequency-shift zero-forcing time-varying equalization for doubly selective channels", *Eurasip Journal on Applied Signal Processing, Special Issue on Reliable Communications over Rapidly Time-Varying Channels*, vol. 2006, ID 47261, 14 pages.

[8] L. Song and J.K. Tugnait, "Doubly-selective fading channel equalization: a comparison of the Kalman filter approach with the basis expansion model-based equalizers," *IEEE Trans. Wireless Commun.*, pp. 60–65, Jan. 2009.

[9] T. Zemen and C.F. Mecklenbrauker, "Time-variant channel estimation using discrete prolate spheroidal sequences," *IEEE Trans. Signal Processing*, pp. 3597–3607, Sep. 2005.

[10] L. Franks, "Polyperiodic linear filtering," in *Cyclostationarity in Commun. and Signal Processing*, edited by W.A. Gardner, IEEE Press, 1994.

[11] S. Haykin, *Adaptive Filter Theory*. New York: Prentice Hall, 1996.

[12] F. Verde, "Subspace-based blind multiuser detection for quasi-synchronous MC-CDMA systems", *IEEE Signal Processing Lett.*, pp. 621-624, July 2004.